Evidence for charge-density-wave nature of the charge-ordered phase in $La_{1/3}Sr_{2/3}FeO_3$

Javier Herrero-Martin,[1] Gloria Subias,[2] Joaquin Garcia,[2,*] Javier Blasco,[2] and M. Concepción Sánchez[2]
[1]*European Synchrotron Radiation Facility, BP 220, 38043 Grenoble Cedex 9, France*
[2]*Departamento de Física de la Materia Condensada, Instituto de Ciencia de Materiales de Aragón, CSIC-Universidad de Zaragoza, Pedro Cerbuna 12, 50009 Zaragoza, Spain*

(Received 24 June 2008; revised manuscript received 22 October 2008; published 27 January 2009)

We have investigated the threefold-charge ordering in $La_{1/3}Sr_{2/3}FeO_3$ sample below $T_{CO}\sim 200$ K. We have measured superlattice reflections, $q=a^*(1/3\ 1/3\ 1/3)$, using the resonant x-ray scattering technique. The nonresonant intensities are consistent with a periodic structural modulation of both Fe and $Sr(La)O_3$ atomic planes. These displacements give rise to two nonequivalent Fe sites in the ratio of 2:1. Strong resonances are observed at the Fe *K* edge in the σ-σ' geometry. These resonances did not exhibit azimuthal dependence. A charge disproportionation of 0.6 electrons is determined between the two Fe sites. Hence, the charge-ordered phase can be better understood as a charge-density-wave with a $\ldots Fe^{3.3+}Fe^{3.9+}Fe^{3.9+}\ldots$ sequence along the cubic [111] direction.

DOI: 10.1103/PhysRevB.79.045121 PACS number(s): 71.30.+h, 71.28.+d, 61.05.C−, 71.45.Lr

I. INTRODUCTION

Metal-insulator transitions in oxides have been the matter of continuous study, particularly in relation to charge ordering (CO) since the discovery of the Verwey transition in magnetite.[1] In mixed-valence oxides of transition metals (*M*), the electric conductivity in the high-temperature phase is commonly explained as due to fast electron hopping between *M* sites with different oxidation states. Upon cooling down to the low-temperature phase, it is proposed that M^{n+} and M^{m+} ions order in specific lattice sites. Such ordering generally localizes the electrons resulting in an abrupt increase in the electrical resistivity below the transition temperature (T_{CO}). This CO model for the insulating phase remains almost unchanged to the present day although experimental evidences are casting doubts on this ionic approximation. The first evidence is the small charge difference between M^{n+} and M^{m+} ions. The subtraction, *m*-*n*, should be an integer number of electrons if the CO model works fine. However, the typical experimental differences are around $0.1-0.2e^-$, far from the predictions of an ionic model.[2–4] These results have been obtained from either bond valence sum structural refinements of diffraction patterns[2,3] or resonant x-ray scattering (RXS) measurements.[3,4] The latter technique is very sensitive to both local structure and valence of the photoabsorbing atom. Second, CO patterns have been found in samples where the M^{n+}/M^{m+} ratio does not agree with the number of different crystallographic sites, i.e., out of stoichiometry.[5,6] In this case, the CO does not match the ionic composition without considering that one of the sites is occupied by two ionic species opposite to the CO driving force. Therefore, the charge disproportionation between different sites does not only seem to be incomplete but unusually small for canonic ionic compounds and new models based on charge-density waves (CDWs) emerge to explain the charge modulation.[7–9]

CO systems where $M^{n+}/M^{m+}=1$ and $m-n=1$ are by far the most studied in the literature. New studies on compounds with a different M^{n+}/M^{m+} ratio and a different electron difference are mandatory to gain insights into the physics of electron localization. The mixed-valence perovskite type $R_{1/3}Sr_{2/3}FeO_3$ (R=La,Pr,Nd) is one of systems that undergo a metal-insulator transition[10] whose transition temperature depends on *R* size. This transition has been classified as CO, and it shows up accompanied by antiferromagnetic spin ordering below 200 K for R=La. Charge disproportionation, which occurs from the paramagnetic average-valence state ($Fe^{3.7+}$) above 200 K to the antiferromagnetic CO state ($Fe^{3+}:Fe^{5+}=2:1$) below that temperature, was originally proposed to explain the metal-insulator transition. Mössbauer spectroscopy detected two kinds of Fe ions with different hyperfine fields.[11] Neutron-powder-diffraction experiments[7,12] suggested that the antiferromagnetic structure of sixfold periodicity was generated from the ordered layers of Fe^{3+} and Fe^{5+} ions in a sequence of $\ldots Fe^{3+}Fe^{3+}Fe^{5+}\ldots$ along the cubic [111] direction. However, no significant differences in the Fe-O bond lengths were observed between the two kinds of Fe cations for these compounds, whereas differences higher than 0.1 Å were found in the related charge disproportionation of $CaFeO_3$.[13] Electron-diffraction measurements identified the superlattice reflections of this CO.[14] However, the physical picture appropriate for the threefold CO phase in $La_{1/3}Sr_{2/3}FeO_3$ is still controversial. First, it is noteworthy that the Fe^{5+} valence is unconventionally high, and second, a recent x-ray absorption spectroscopy study in the $La_{1-x}Sr_xFeO_3$ series has discarded a charge disproportionation of the type $2Fe^{4+}\rightarrow Fe^{3+}+Fe^{5+}$ for $La_{1/3}Sr_{2/3}FeO_3$. The mixed-valence state of the Fe atom in this sample is either a pure intermediate Fe^{3x+} or a mixture of Fe^{3+} and Fe^{4+}.[15]

RXS experiments at the metal K edge have demonstrated the capability of this technique to discriminate the type and magnitude of the charge disproportionation in many CO transition-metal oxides where the charge disproportionation is related to differences in the metal-oxygen coordination distances. This occurs because different charge states of the transition-metal cation are directly related to different ionic radii. Indeed, this has been the case of half-doped manganites,[4,5] Fe_3O_4,[2] $NdNiO_3$,[16] and $CaFeO_3$.[17] The x-ray scattering intensity at the CO superlattice reflections will be enhanced as the incident x-ray energy is tuned to the metal K

edge due to the difference in the anomalous scattering factor of the resonant M atoms with different electronic states.

In this paper, we use the RXS technique to investigate the CO periodicity with $q=a^*(1/3\ 1/3\ 1/3)$ in the $La_{1/3}Sr_{2/3}FeO_3$ iron perovskite. If the CO followed the formal valence state, the new lattice would have a period three times larger than the disordered phase, so the study was focused on superlattice reflections of the type $(h/3\ h/3\ h/3)_p$, where the p subscript stands for primitive cubic perovskite structure. A complementary measurement of these reflections was also performed by conventional single-crystal x-ray diffraction XRD. $La_{1/3}Sr_{2/3}FeO_3$ is not cubic but it has a rhombohedral distortion which is usually described in a hexagonal lattice (R-3c space group). However, the pseudocubic cell is widely used in the literature, and we have followed here this approximation. We recall that [1 1 1] cubic and [0 0 1] hexagonal directions are equivalent. The Fe K edge RXS spectra measured on these superlattice reflections that are weak off-resonance are extremely sensitive to subtle displacements of any atom in the unit cell due to the interference of the resonant contrast with the Thomson scattering. In this way, we have determined the structural modulation of the Fe and $Sr(La)O_3$ atomic planes along the cubic [1 1 1] direction and quantitatively estimate the charge segregation between the two distinct charge states originated by this structural modulation.

II. EXPERIMENTAL METHOD

Single crystals of $La_{1/3}Sr_{2/3}FeO_3$ were grown by the floating zone method.[18] The crystals were carefully investigated by x-ray powder diffraction and electrical and magnetic measurements exhibiting the same behavior as previously reported.[15,18] A large crystal was cut and polished with the cubic [1 1 1] direction as the surface normal for RXS experiments. A small crystal taken from the same batch was used in the XRD experiments. RXS experiments at the Fe K edge were undertaken at the ID20 beamline[19] of the ESRF, Grenoble, France. The x-rays were monochromatized by a Si(111) double-crystal system with an energy resolution of 0.7 eV. The sample was mounted on the four circle vertical diffractometer, which allows us to perform azimuthal scans. The incident beam was polarized perpendicular to the scattering plane (σ), and a MgO (220) crystal was used for polarization analysis of the scattered signal. The use of a closed-cycle refrigerator limited the base sample temperature to 10 K. The energy scans were recorded by adjusting the diffractometer to keep the momentum transfer fixed at each energy but integrated intensity measurements by rocking the sample through the reflections were not performed. To check the reliability of the Thomson intensities, nonresonant intensity data of the $(h/3\ h/3\ h/3)_p$ reflections were collected at 120 K on a four circle Xcalibur diffractometer with graphite monochromatized Mo K_α radiation ($\lambda=0.71073$ Å).

III. RESULTS

Figure 1 shows the energy dependence of the RXS intensity of the $(2/3\ 2/3\ 2/3)_p$, $(4/3\ 4/3\ 4/3)_p$, and $(5/3\ 5/3\ 5/3)_p$ reflections with σ-σ' polarization in the insulating state at 10 K. The x-ray absorption spectrum is depicted in Fig. 1(b) as energy reference. We observe the nonresonant Thomson scattering at energies below the Fe K edge. These reflections are forbidden in both cubic (Pm-3m) and rhombohedral (R-3c) symmetries. They must arise from collective motion of the Fe and $Sr(La)O_3$ atomic planes along the $[1\ 1\ 1]_p$ direction. Note that any displacement perpendicular to that direction does not contribute to the scattering of (hhh) reflections. The resonant scattering for the $(4/3\ 4/3\ 4/3)_p$ and $(5/3\ 5/3\ 5/3)_p$ reflections has a significant peak (maximum) at $E=7129.5$ eV, approximately 3 eV above the Fe K edge. However, it strongly drops (minimum) at the same energy for the $(2/3\ 2/3\ 2/3)_p$ reflection. Scattered intensity was not observed in the σ-π' channel for any of the studied reflections. No indication of azimuthal dependence was found from the measurements of the three reflections, as shown in the inset of Fig. 1(b) for $(4/3\ 4/3\ 4/3)_p$. Moreover, the curves of energy scans at different azimuth angles can be superimposed to each other (not shown). This reveals that Fe atoms have not a local anisotropy in the present case and their anomalous scattering factors can be considered as a scalar. Furthermore, this result discards the presence of orbital ordering along this direction. Figure 2 shows the temperature evolution of the resonant peak intensity for $(4/3\ 4/3\ 4/3)_p$ and $(5/3\ 5/3\ 5/3)_p$ re-

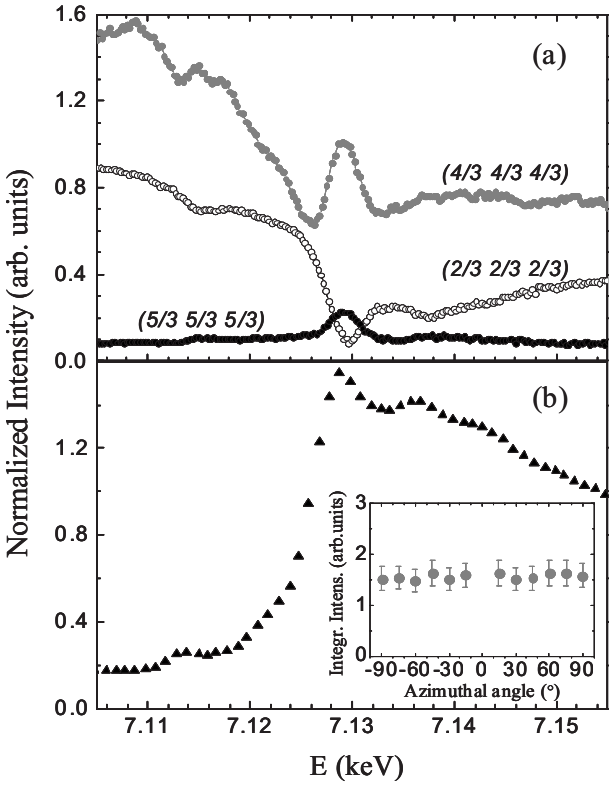

FIG. 1. (a) The energy dependence of the intensity of the $(2/3\ 2/3\ 2/3)_p$, $(4/3\ 4/3\ 4/3)_p$, and $(5/3\ 5/3\ 5/3)_p$ reflections taken at 10 K with σ-σ' polarization as measured (no self-absorption correction). (b) The x-ray absorption spectrum near the Fe K edge. Inset shows the azimuthal angle dependence of the RXS intensity of the $(4/3\ 4/3\ 4/3)_p$ reflection at 7129.5 eV.

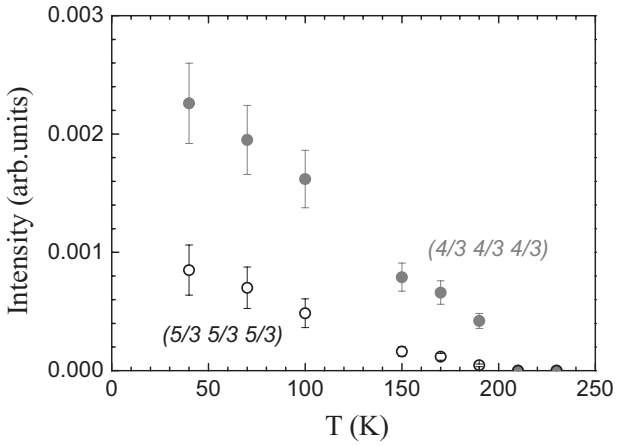

FIG. 2. Temperature dependence (heating) of the integrated intensity of the $(4/3\ 4/3\ 4/3)_p$ and $(5/3\ 5/3\ 5/3)_p$ reflections at the energy of 7129.5 eV.

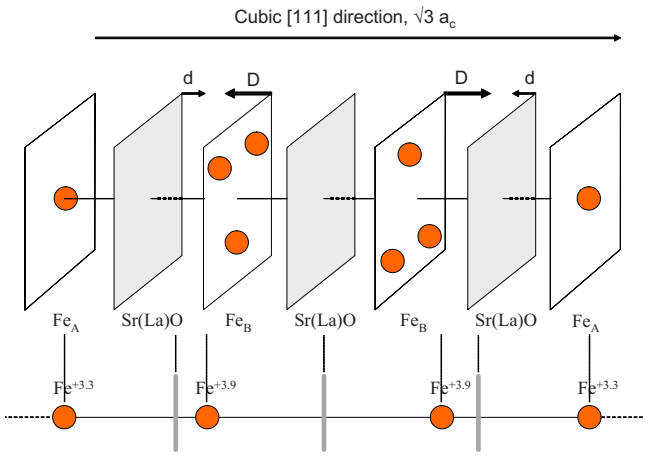

FIG. 3. (Color online) Schematic picture showing the displacements of Fe (D) and Sr(La)O_3 (d) atomic planes on the $[1\ 1\ 1]_p$ direction derived from our refinement of the nonresonant intensities and the charge-density-wave modulation with respect to one-half of the magnetic supercell. The atomic shifts have been exaggerated for the sake of clarity.

flections, which gradually decreases by increasing the temperature, and it completely vanishes at $T_{CO}=200$ K. This temperature dependence indicates that $(h/3\ h/3\ h/3)_p$ reflections come from a threefold periodicity in the insulating phase with respect to the simple perovskite.

These results agree with the occurrence of charge disproportionation where Fe atoms are splitted in two distinct crystallographic sites with a periodicity $Fe_AFe_BFe_B$ along the $[1\ 1\ 1]_p$ direction. Such a disproportionation will create a periodic structural distortion in the crystal.

IV. DISCUSSION AND CONCLUSIONS

It is worth discussing the nonresonant (Thomson) scattering of these $(h/3\ h/3\ h/3)_p$ reflections to determine the lattice modulation. Figure 1(a) reveals strong variation in the Thomson scattering (below the absorption edge) among the different satellite reflections. This fact cannot be accounted only with displacements of the Fe atoms since a monotonous behavior of the Thomson intensity with increasing the h index should be observed. Therefore, simultaneous displacements of the Fe, Sr(La), and O atomic planes are necessary. As the $(h/3\ h/3\ h/3)_p$ structure factors depends exclusively on small displacements of the atoms along the $[1\ 1\ 1]_p$ direction, one-dimensional structural models in this direction can approach the energy-dependent RXS intensity for $(h/3\ h/3\ h/3)$ reflections at different h indices. Considering the body diagonal of the cubic perovskite, we got a threefold linear sequence of Fe and Sr(La)O_3 planes intercalated as shown in Fig. 3. At first, we constraint the Sr(La)O_3 planes to move rigidly. Among the possible types of atomic shifts, those where both Fe and La(Sr)O_3 planes are moved in phase give rise to a monotonous evolution of the Thomson intensity and a resonant peak for all the $(h/3\ h/3\ h/3)_p$ reflections, opposite to the experimental results [see Fig. 1(a)]. To qualitatively reproduce the experiment it is necessary that the Fe and the La(Sr)O_3 planes were moved in opposite directions, keeping the inversion symmetry of the supercell (triple perovskite). There are two models that reproduce the experimental facts. One is depicted in Fig. 3 and the other is the contrary (inverted arrows). As it is shown in Fig. 3, Fe and Sr(La)O_3 planes move in opposite to each other giving rise to a shift of two Fe atoms away from the center of their surrounding octahedron of oxygen atoms. These shifts produce an ordered sequence of two compressed Fe_BO_6 and one expanded Fe_AO_6 octahedron along the $[1\ 1\ 1]_p$ direction as observed in related triple perosvkites.[20] The Fe_BO_6 octahedron is asymmetric with three short Fe-O distances and three large Fe-O bond lengths. The Fe_AO_6 octahedron instead is regular. The other model will give the complementary sequence (one compressed and two expanded iron sites). Since our previous absorption results[15] impose the existence of two Fe in a higher valence state (shorter Fe-O mean bond length) and one Fe in a lower valence state (longer Fe-O mean bond length), only the two compressed and one expanded iron-sites model is compatible with both x-ray absorption and RXS data. In the following, we will refer to this model.

In order to give a quantitative estimation of the atomic displacements along the $[1\ 1\ 1]_p$ direction and the charge segregation, we fit the RXS spectra of the three $(h/3\ h/3\ h/3)_p$ reflections using the proposed model. The structure factors of these reflections are then given in the linear approach by

$$F(Q,E) = 4\pi h\left[Df^0_{\mathrm{Fe}} \sin\left(\frac{2\pi}{3}h\right) - df^0_{\mathrm{La,Sr,O}} \sin\left(\frac{\pi}{3}h\right)\right] + 4\pi h d f^{\mathrm{anom}}_{\mathrm{Fe}} \sin\left(\frac{2\pi}{3}h\right) + \Delta f^{\mathrm{anom}}_{\mathrm{Fe}},$$

where f^0_{Fe} and $f^0_{\mathrm{La,Sr,O}}$ are the Thomson scattering factors of Fe and Sr(La)O_3 planes, $f^{\mathrm{anom}}_{\mathrm{Fe}} = f'_{\mathrm{Fe}_B}(E) + i f''_{\mathrm{Fe}_B}(E)$ is the anomalous scattering factor for the Fe_B atomic planes, and $\Delta f^{\mathrm{anom}}_{\mathrm{Fe}}(E) = f'_{\mathrm{Fe}_A}(E) - f'_{\mathrm{Fe}_B}(E) + i[f''_{\mathrm{Fe}_A}(E) - f''_{\mathrm{Fe}_B}(E)]$, being $f'_{\mathrm{Fe}_i}(E)$ and $f''_{\mathrm{Fe}_i}(E)$ as the real and imaginary parts of the anomalous factor, respectively. The first term corresponds to the Thomson contribution due to the displacements of the Fe

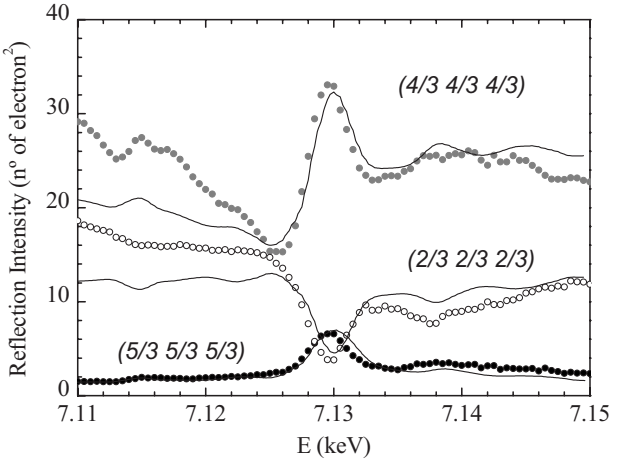

FIG. 4. Energy-dependent RXS intensity of the $(h/3\ \ h/3\ \ h/3)_p$ reflections (circles) compared with the best-fitted curves (solid lines) simulated as described in the text.

(D) and Sr(La)O_3 (d) planes; the second term is the anomalous contribution due to the Fe_B motion and the third term comes from the difference between the anomalous scattering factors of the two types of Fe atoms (A and B in Fig. 3). The first term is positive for $h=4/3$ and 5/3 and negative for $h=2/3$. This change in sign depending on the reflection arises from the opposite motion of the La(Sr)O_3 atoms with respect to the Fe ones, which makes their Thomson scattering factor to be either in phase or out of phase with the Thomson scattering factor of the Fe atoms. Since the intensity of the reflections are given by $|F(Q,E)F^*(Q,E)|$, the crossed term between the Thomson scattering and $\Delta f_{\mathrm{Fe}}^{\mathrm{anom}}(E)$ will produce either a peak or a valley at the energy of the resonance as was also reported in the RXS study of related cobaltites.[21]

We will now model the anomalous scattering factors of the two types of Fe atoms. We note that the nonpolarized x-ray absorption spectrum is proportional to the sum $f''_{\mathrm{Fe}_A}(E)+2f''_{\mathrm{Fe}_B}(E)$. From the experimental absorption spectrum and the Kramers-Kronig relation, the real and imaginary parts of the scattering factor of the Fe atom with formal average valence of 3.67 are obtained. It is well known that the K-edge energy (E_0) shifts to higher values for higher valence states in an almost linear dependence.[15] Thus, we have rigidly displaced these real and imaginary parts by $E_0-2\delta$ and $E_0+\delta$ to simulate the effect of the valence state on the site-selective scattering factors of the Fe_A and Fe_B sites with 3δ the chemical shift for the two different electronic states.

Fits to the resonant scattered intensity of the $(2/3\ \ 2/3\ \ 2/3)_p$, $(4/3\ \ 4/3\ \ 4/3)_p$, and $(5/3\ \ 5/3\ \ 5/3)_p$ reflections were carried out by the least-squares minimization method of three adjustable parameters. These parameters stand for Fe (D) and La(Sr)O_3 (d) displacements and for the chemical shift between the two sites (3δ). The simulated RXS intensities reproduce rather well the experimental energy dependence of the three reflections, as shown in Fig. 4. Although the intensity below the absorption edge is not as good as we expected, the fits nicely reproduces the main features of the spectra. The refined displacements were $D(\mathrm{Fe})=0.013$ Å and $d(\mathrm{SrLaO_3})=0.0054$ Å. In order to test these atomic displacements, linear scans along the $[1\ \ 1\ \ 1]_p$ direction were collected by single-crystal XRD from the $(2/3\ \ 2/3\ \ 2/3)_p$ up to $(7/3\ \ 7/3\ \ 7/3)_p$ reflections. Our experimental setup clearly detected both $(2/3\ \ 2/3\ \ 2/3)_p$ and $(4/3\ \ 4/3\ \ 4/3)_p$ reflections but it fails to observe the very weak $(5/3\ \ 5/3\ \ 5/3)_p$ and $(7/3\ \ 7/3\ \ 7/3)_p$ ones. The detection of the $(5/3\ \ 5/3\ \ 5/3)_p$ in the RXS measurements was possible due to the high brilliance of a synchrotron radiation source. Table I compares the integrated intensities of the observed reflections by single-crystal XRD to those obtained from the proposed pseudo-one-dimensional structural model (I_{calc}). Correlation between calculated and experimental intensities is quite good, supporting our model of atomic shifts as a reasonable approach to the real atomic arrangement in the low-temperature phase.

TABLE I. Observed (single-crystal XRD) and calculated intensity for the low-temperature modulated structure of $La_{1/3}Sr_{2/3}FeO_3$ based on the atomic displacements shown in Fig. 3 with $D=0.013$ Å and $d=0.0054$ Å. Estimated error for I_{obs} are given in parentheses.

hkl	I_{obs}	I_{calc}
2/3 2/3 2/3	9.6(4)	12.2
4/3 4/3 4/3	26.2(4)	23.8
5/3 5/3 5/3	0(4)	1.3
7/3 7/3 7/3	0(4)	3.6

Concerning the chemical shift between the two types of Fe cations, the energy shift between Fe_A and Fe_B is found to be 0.7 ± 0.1 eV. This value can be compared to the energy shift[15] of 1.26 eV between Fe^{3+} and Fe^{4+}, and assuming a linear relationship between chemical shift and local charge, it results in a charge difference of $q\approx0.6\pm0.2e^-$ between both atoms. This value is much smaller than that proposed by Mössbauer spectroscopy, in which Fe_A and Fe_B were attributed to Fe^{5+} and Fe^{3+}, respectively. However, similar qualitative results are obtained. Above T_{CO}, there is a regular octahedron which is split up in two kinds of octahedra below T_{CO}: the asymmetric compressed Fe_BO_6 and the expanded Fe_AO_6. The two types of octahedra should have two different hyperfine fields. Therefore, we suggest that a better description of the low-temperature phase is the presence of a commensurate CDW, which results from the addition of two modulations, the pairing of the Fe atomic planes and the pairing of the Sr(La)O_3 atomic planes. Accordingly, there is a charge difference between the "compressed" octahedron (Fe_B atoms in Fig. 3) and the "expanded" octahedron (Fe_A atoms) in the ratio of 2:1. The CDW ordering would be $Fe^{3.3+}Fe^{3.9+}Fe^{3.9+}Fe^{3.3+}Fe^{3.9+}Fe^{3.9+}$. We would like to note that the estimated valence is formal, based on the assumption that Fe is 3+ and 4+ in the $LaFeO_3$ and $SrFeO_3$ reference compounds, respectively. The extrapolation of these formal valences to $3d$ occupation at the iron atom is constrained to the assumption that formal Fe^{3+} and Fe^{4+} have integer $3d^5$ and $3d^4$ electronic configurations, respectively. However, soft x-ray absorption experiments[22] have shown that none of the two references can be described as a unique $3d^n$ configuration but with mixture of $3d^n$ and $3d^{n+1}L$ configurations.

Therefore, care must be taken in order to translate formal ionic valences into number of 3*d* electrons for these compounds.

In conclusion, we have observed charge disproportionation ($Fe^{3.66-2q/3}$ and $Fe^{3.66+q/3}$ in the ratio of 1:2) at the metal-insulator transition in $La_{1/3}Sr_{2/3}FeO_3$ using RXS. Such disproportion is originated from a quasi-one dimensional structural modulation similar to that found in classical charge-density-wave systems, as already proposed for other CO compounds.[8,9] In this case, we can distinguish two coupled modulations; one arises from the Fe atomic planes and the other from the $Sr(La)O_3$ atomic planes. The decoupling of the Sr(La) and O motions in the $[1\ 1\ 1]_p$ direction and possible transversal modulations cannot be discarded. These structural modulations differentiate two crystallographic sites for the Fe atoms with different local charges. RXS has allowed us to determine the local charge on each of the two Fe sites showing that the amount of the charge segregation is only $0.6e^-$, quite similar to other mixed-valence *M* oxides.[2–6,15] The oxygen atoms also present a structural threefold modulation. Therefore, we cannot discard a CDW in the oxygen sites due to the strong hybridization between the Fe 3*d* and O 2*p* bands.[22] The two different magnetic moments refined from neutron-diffraction data and the two different Mössbauer spectra observed below the metal-insulator transition are explained as due to the differentiation into two different crystallographic sites; one of them with asymmetric octahedral environment, but the formal valence states for both iron cations are nonintegral.

ACKNOWLEDGMENTS

This work was supported by the Spanish CICyT Project No. MAT2005-04562 and Diputación General de Aragón (DGA-CAMRADS). The authors thank ESRF for granting beam time and B. Diosdado for her assistance in the XRD experiments.

*Corresponding author. Instituto de Ciencia de Materiales de Aragón, CSIC-Universidad de Zaragoza, C/Pedro Cerbuna 12, 50009 Zaragoza, Spain.jgr@unizar.es

[1] E. J. W. Verwey, Nature (London) **144**, 327 (1939).
[2] J. P. Wright, J. P. Attfield, and P. G. Radaelli, Phys. Rev. B **66**, 214422 (2002).
[3] J. García and G. Subías, J. Phys.: Condens. Matter **16**, R145 (2004).
[4] J. Herrero-Martín, J. García, G. Subías, J. Blasco, and M. Concepcion Sanchez, Phys. Rev. B **70**, 024408 (2004).
[5] S. Grenier, J. P. Hill, D. Gibbs, K. J. Thomas, M. v. Zimmermann, C. S. Nelson, V. Kiryukhin, Y. Tokura, Y. Tomioka, D. Casa, T. Gog, and C. Venkataraman, Phys. Rev. B **69**, 134419 (2004).
[6] G. Subías, M. C. Sánchez, J. García, J. Blasco, J. Herrero-Martín, C. Mazzoli, P. Beran, M. Nevriva, and J. L. García-Muñoz, J. Phys.: Condens. Matter **20**, 235211 (2008).
[7] P. D. Battle, T. C. Gibb, and P. Lightfoot, J. Solid State Chem. **84**, 271 (1990).
[8] J. C. Loudon, S. Cox, A. J. Williams, J. P. Attfield, P. B. Littlewood, P. A. Midgley, and N. D. Mathur, Phys. Rev. Lett. **94**, 097202 (2005).
[9] R. J. McQueeney, M. Yethiraj, W. Montfrooij, J. S. Gardner, P. Metcalf, and J. M. Honig, Phys. Rev. B **73**, 174409 (2006).
[10] S. K. Park, T. Ishikawa, Y. Tokura, J. Q. Li, and Y. Matsui, Phys. Rev. B **60**, 10788 (1999).
[11] M. Takano, J. Kawachi, N. Nakanishi, and Y. Takeda, J. Solid State Chem. **39**, 75 (1981).
[12] J. B. Yang, X. D. Zhou, A. Chu, W. M. Hikal, Q. Cai, J. C. Ho, D. C. Kundaliya, W. B. Yelon, W. J. James, H. U. Anderson, H. H. Hamdeh, and S. K. Malik, J. Phys.: Condens. Matter **15**, 5093 (2003).
[13] P. M. Woodward, D. E. Cox, E. Moshopoulou, A. W. Sleight, and S. Morimoto, Phys. Rev. B **62**, 844 (2000).
[14] J. Q. Li, Y. Matsui, S. K. Park, and Y. Tokura, Phys. Rev. Lett. **79**, 297 (1997).
[15] J. Blasco, B. Aznar, J. García, G. Subías, J. Herrero-Martín, and J. Stankiewicz, Phys. Rev. B **77**, 054107 (2008).
[16] U. Staub, G. I. Meijer, F. Fauth, R. Allenspach, J. G. Bednorz, J. Karpinski, S. M. Kazakov, L. Paolasini, and F. d'Acapito, Phys. Rev. Lett. **88**, 126402 (2002).
[17] T. Akao, Y. Azuma, M. Usuda, Y. Nishihata, J. Mizuki, N. Hamada, N. Hayashi, T. Terashima, and M. Takano, Phys. Rev. Lett. **91**, 156405 (2003).
[18] J. Blasco, M. C. Sánchez, J. García, J. Stankiewicz, and J. Herrero-Martin, J. Cryst. Growth **310**, 3247 (2008).
[19] L. Paolasini, C. Detlefs, C. Mazzoli, S. Wilkins, P. P. Deen, A. Bombardi, N. Kernavanois, F. de Bergevin, F. Yakhou, J. P. Valade, I. Breslavetz, A. Fondacaro, G. Pepellin, and P. Bernard, J. Synchrotron Radiat. **14**, 301 (2007).
[20] V. Ting, Y. Liu, L. Noren, R. L. Withers, D. J. Goossens, M. James, and C. Ferraris, J. Solid State Chem. **177**, 4428 (2004).
[21] J. Blasco, J. García, G. Subías, H. Renevier, M. Stingaciau, K. Conder, and J. Herrero-Martin, Phys. Rev. B **78**, 054123 (2008).
[22] M. Abbate, F. M. F. de Groot, J. C. Fuggle, A. Fujimori, O. Strebel, F. Lopez, M. Domke, G. Kaindl, G. A. Sawatzky, M. Takano, Y. Takeda, H. Eisaki, and S. Uchida, Phys. Rev. B **46**, 4511 (1992).